RSC Advances

ROYAL SOCIETY OF CHEMISTRY

www.rsc.org/advances

Carbon dots in magnetic colloidal nanocrystal clusters

The existence of carbon dots is revealed inside and on the surface of magnetic colloidal nanocrystal clusters in a typical hydrothermal synthesis process.

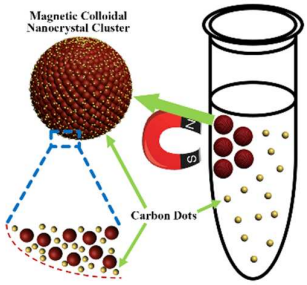

RSC Advances

RSCPublishing

COMMUNICATION

Carbon dots in magnetic colloidal nanocrystal clusters

Cite this: DOI: 10.1039/xoxxoooooox

Ye Liu, Ye Tian and Wuli Yang*

Received ooth January 2014,
Accepted ooth January 2014

DOI: 10.1039/xoxxoooooox

www.rsc.org/

In this study, carbon dots are found to be fabricated simultaneously during the typical hydrothermal synthesis process of magnetic colloidal nanocrystal clusters (MCNCs). Their existence in the solvent (ethylene glycol), on the surface and in the interior of MCNCs is also revealed.

Carbon dots (CDs), as a new type of fluorescent nanomaterials, have attracted tremendous attention in the recent years because of their potential applications in bioimaging,[1,2] medical diagnosis,[3] optoelectronic devices,[4,5] sensors[6] and catalysis.[7] Compared to organic dyes and fluorescent semiconductor nanocrystals, CDs provide many promising advantages such as bright fluorescence, low photobleaching, robust chemical inertness and excellent biocompatibility.[8] Currently, various methodologies have been developed to prepare CDs, such as arc discharge, laser ablation, electrochemical oxidation, and hydrothermal method.[9] Among these strategies, hydrothermal synthesis of CDs has become more and more popular due to low cost, easy operation and abundant resources. Nearly all organics could be used as carbon sources such as citric acid, ethylene diamine, polyethylene glycol, and L-ascorbic acid.[10-14]

Magnetic colloid nanocrystal clusters (MCNCs) have arouse great interest and desire of exploration in biomedical applications: magnetic resonance imaging, proteins/peptides enrichment and detection, biomarker detection and targeted drug delivery.[15] As known, in a typical hydrothermal synthesis process of MCNCs, Fe^{3+} ions undergo a sodium acetate (NaOAc)-promoted hydrolysis and then are partially reduced to magnetite (Fe_3O_4) nanoparticles by ethylene glycol with the assistance of trisodium citrate. The magnetite nanoparticles then generally aggregate into clusters (MCNCs) at high temperature.[16] It is reasonable to hypothesize that when trisodium citrate and ethylene glycol are hydrothermally treated, CDs are fabricated simultaneously during the synthesis process of MCNCs. In this work, the hypothesis is proved and the existence of CDs in the system is confirmed. Also, the exact locations of CDs and the structure of MCNCs are also discussed: CDs are revealed to be not only dispersed in the solvent, but also stuck on the surface and embedded in the interior of MCNCs. This research offers new insights into the preparation of CDs and the architecture of MCNCs.

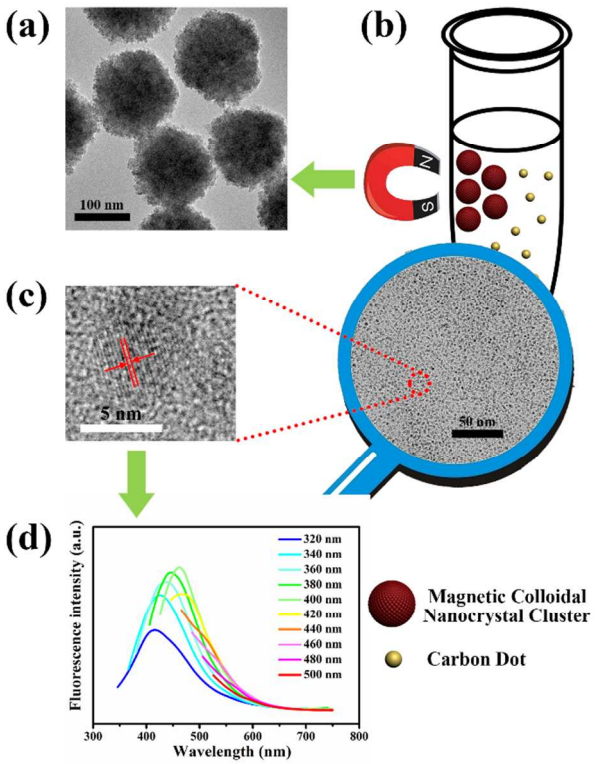

Figure 1 (a) TEM image of MCNCs. (b) Schematic illustration of the as-prepared mixture and TEM image of CDs in the solvent. The diagram is not drawn to scale. (c) HRTEM image of a carbon dot. (d) PL emission spectra of CDs in the solvent at different excitation wavelengths.

Firstly, MCNCs are fabricated in a typical hydrothermal strategy (Figure 1a), and numerous CDs are observed in the as-prepared mixture (schemed in Figure 1b). From the transmission electron microscopy (TEM) image of CDs in the solvent (ethylene glycol), it can be seen that large amounts of CDs with size of about 5 nm are dispersed well in ethylene glycol (Figure 1b). High-resolution TEM (HRTEM) measurement (Figure 1c) reveals that CDs are graphitic in

nature with a lattice spacing of 0.220 nm consistent with (100) facet of graphite.[9] Raman spectroscopy is used to confirm the quality of the CDs (Figure S1 in the Supporting Information). Two major features, D band and G band, are observed at around 1385 and 1575 cm^{-1}, respectively. The relative intensity of the "disorder" D-band and the crystalline G-band (I_D/I_G) for the CDs is about 1.23.[4] Moreover, after careful removal of MCNCs with a magnet, nuclear magnetic resonance (NMR, ^1H and ^{13}C) of the CDs is employed to distinguish sp^2- and sp^3-hybridized carbon atoms (Figure S2 in the Supporting Information). In the ^{13}C NMR spectrum, signals in the range of 20-70 ppm, which correspond to aliphatic (sp^3) carbon atoms, and signals from 100 to 185 ppm, which are indicative of sp^2 carbon atoms, are observed. Among them, signals in the range of 170-185 ppm, which correspond to carboxyl groups, are also present.[17] The surface groups are also investigated by X-ray photoelectron spectroscopy (XPS) analysis (Figure S3a, b in the Supporting Information). C1s analysis reveals several different types of carbon atoms: graphitic or aliphatic (C=C and C-C), C-O, C=O and O=C-O.[18] In the photoluminescence (PL) emission spectra of the as-prepared mixture, the excitation-dependent PL behaviour is observed, which is common in primarily reported CDs (Figure 1d).[8] Moreover, their ultraviolet/visible (UV/vis) spectrum is similar to that of CDs (Figure S4 in the Supporting Information). All the above results prove the existence of CDs in the solvent.

In addition, the PL emission spectra of MCNCs present an excitation-dependent behaviour (Figure S5 in the Supporting Information), and washing with deionized water dramatically decreases the fluorescence of MCNCs, indicating the CDs are weakly absorbed on the surface of MCNCs (Figure S6 in the Supporting Information). However, in the Raman spectrum of MCNCs after ten times washing, D and G bands can still be observed, suggesting the existence of CDs in the system (Figure S1 in the Supporting Information). In this case, to further release CDs on the surface, dopamine is selected to exchange with CDs due to the binding preference of catechol groups toward Fe^{3+} ions (schemed in Figure 2a).[19, 20] After the ligand exchange, the UV/vis absorption spectrum shows an absorption band at 262 nm, which belongs to the absorption of dopamine (Figure S7 in the Supporting Information). The Fourier transform infrared (FTIR) spectra of MCNCs and MCNC-dopamine are also recorded (Figure S8 in the Supporting Information). Compared to MCNCs, it can be seen that the MCNC-dopamine have an absorption peak at 1268 cm^{-1} associated with the C-OH stretching mode of the phenolic hydroxyl groups. Thermo gravimetric analysis (TGA) in N_2 of MCNC-dopamine shows a larger weight loss of about 15% in the range of 100~800 ^oC while the MCNCs only have a weight loss of 12%, revealing that the former contains more organic groups (Figure S9 in the Supporting Information). Furthermore, the zeta potential of MCNCs changes from -14.8 mV to zero after the dopamine grafting (Table S1 in the Supporting Information), implying the increase of surface positive charge density of MCNCs attributed to the amine groups. In a word, these results prove that dopamine has been successfully grafted onto the surface of MCNCs.

After the ligand exchange, CDs are observed in the supernatant. Figure 2b shows the TEM image of CDs with a mean size of about 4 nm. The crystalline structure of CDs with the lattice spacing of 0.205 nm is proved by the HRTEM image shown in Figure 2b (inset), which corresponds well to the in-plane lattice spacing of graphite (102 facet).[9] The supernatant also shows an excitation-dependent behavior in the PL emission spectra (Figure 2c). The release of CDs in the ligand exchange process confirms that CDs are attached to the surface of MCNCs. As known, CDs contain many -OH and -COOH moieties on their surface, which have strong coordination affinity to Fe^{3+} ions. As a result, CDs are attached to the surface of MCNCs through coordination in the synthesis process. Whereas the fluorescence of CDs was quenched by Fe^{3+} ions on account of the nonradiative electron-transfer between Fe^{3+} ions and -OH,-COOH moieties (Figure S6 in the Supporting Information).[10] Upon the addition of dopamine, the stronger interaction between Fe^{3+} ions and catechol groups disturbed the interaction between Fe^{3+} ions and CDs, which leaded to the release of CDs from the surface of MCNCs (Figure 2a).

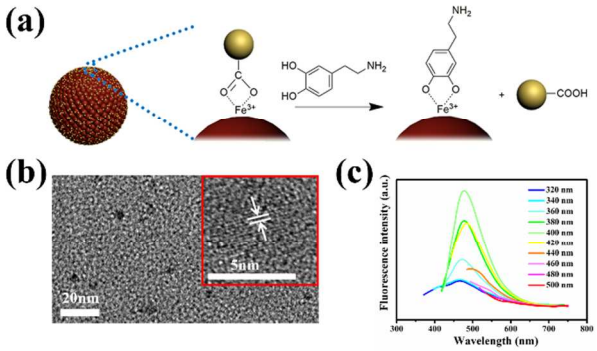

Figure 2 (a) Schematic illustration of CD release in the ligand exchange process. (b) TEM image of CDs released from the surface of MCNCs. Inset: HRTEM image. (c) PL emission spectra of CDs released form the surface of MCNCs at different excitation wavelengths.

Then Fe_3O_4 composition in the MCNCs is etched by diluted hydrochloric acid and sodium hydroxide is added to precipitate Fe^{3+} and Fe^{2+} ions. CDs are observed in the solution after etching. The TEM image shows CDs with a diameter of about 4 nm (Figure 3b). HRTEM image reveals the high crystallinity of CDs with the lattice spacing of 0.185 nm which agrees well with the (105) facet of graphite (Figure 3b, inset).[9] The excitation-dependent behavior is displayed in the PL emission spectra of CDs (Figure 3c). The release of CDs in the etching process brings out the fact that CDs exist in the interior of MCNCs. According to previous reports, the MCNCs undergo a two-stage growth process in which the primary nanoparticles nucleate first in a supersaturated solution and then aggregate into clusters at high temperature.[16, 21] Considering the strong coordination affinity of -OH,-COOH moieties with Fe^{3+} ions, CDs are able to anchor on the surface of the primary nanoparticles, and thus embedded in the interior of the MCNCs (Figure 3a). Namely, the MCNCs are composed of Fe_3O_4 nanocrystals and CDs. Since the CDs are surrounded by Fe_3O_4 nanocrystals, their fluorescence is also quenched by Fe^{3+} ions as mentioned above.[10]

It should be noted that owing to the different growing environment, the CDs obtained from the solvent, ligand exchange and etching process have various size and lattice fringe. To further investigate the difference, Raman spectroscopy (Figure S1 in the Supporting Information) and XPS analysis (Figure S3 in the Supporting Information) are conducted. XPS analysis of the three kinds of CDs presents diverse compositions of carbon elements, while the I_D/I_G values measured in the Raman spectroscopy are similar. With a similar carbon-lattice-structure content (indicated by I_D/I_G values), the PL emission spectra of the three kinds of CDs are alike.

Inspired by the above results, the MCNCs are dispersed in a pH 4 buffer, which simulates physiological environment. Likewise, CDs can be observed in the solution after the etching process. The TEM image shows CDs with an average size about 4 nm (Figure 4a). The HRTEM image proves the high crystallinity of CDs with the lattice spacing around 0.210 nm, which corresponds with the (100) diffraction planes of graphite (Figure 4a, inset).[9] The PL emission

spectra show a typical fluorescent properties of CDs, while the fluorescence intensity is somewhat weak (Figure 4b).

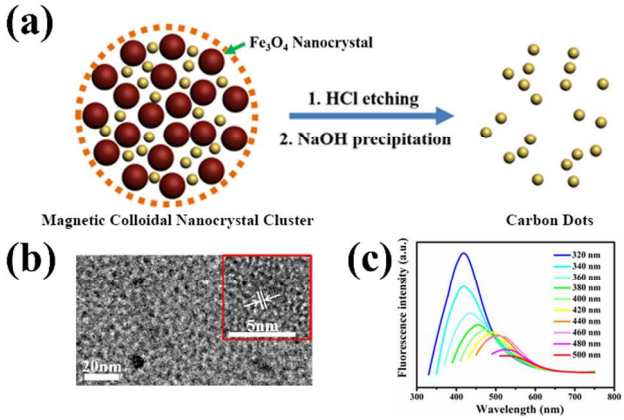

Figure 3 (a) Schematic illustration of the architecture that the MCNCs are composed of Fe_3O_4 nanoparticles and CDs and the etching process. The diagram is not drawn to scale. (b) TEM image of CDs released from the interior of MCNCs with hydrochloric acid etching. Inset: HRTEM image. (c) PL emission spectra of CDs released from the interior of MCNCs at different excitation wavelengths.

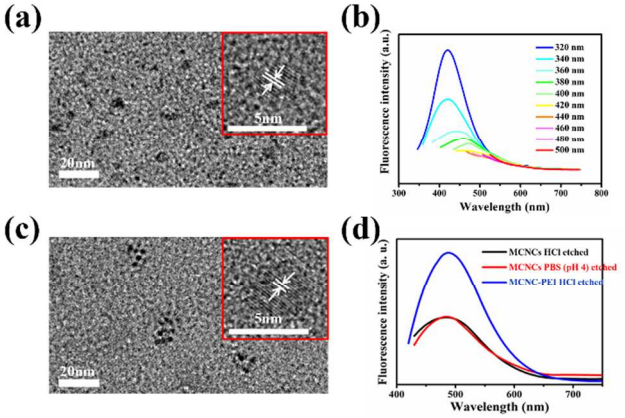

Figure 4 (a) TEM image of CDs released from the interior of MCNCs with pH 4 buffer etching. Inset: HRTEM image. (b) PL emission spectra of CDs released from the interior of MCNCs at different excitation wavelengths. (c) TEM image of CDs released from MCNC-PEI composites with hydrochloric acid etching. Inset: HRTEM image. (d) Comparison of fluorescence intensity of CDs released from MCNCs or MCNC-PEI composites with hydrochloric acid and pH 4 buffer etching.

To increase the fluorescence intensity, polyethylene imine (PEI) is chosen to graft onto the MCNCs, since PEI contains a great amount of amine groups which can improve the fluorescence quantum yield of CDs.[10] To verify the successful grafting of PEI onto the surface of MCNCs, TGA analysis of the composites is conducted. Compared with pure MCNCs, the MCNC-PEI composites have a larger weight loss, implying more organic groups (Figure S9 in the Supporting Information). Moreover, the zeta potential (Table S1 in the Supporting Information) shows the changes from -14.8 mV to 20.8 mV after grafting PEI. These results prove the efficient grafting of PEI onto the surface of MCNCs. When MCNC-PEI composites are etched with hydrochloric acid, CDs are observed in the solution. Figure 4c shows the TEM and HRTEM images of CDs, which reveal CDs with a diameter of about 4 nm (Figure 4c). The same lattice spacing of around 0.194 nm agrees well with the (104) spacing of graphite (Figure 4c, inset).[9] As expected, the fluorescence intensity of CDs released from the MCNCs increases drastically after the grafting (Figure 4d).

In summary, CDs are fabricated simultaneously during the typical hydrothermal synthesis process of MCNCs. Firstly, CDs exist in the solvent and weakly absorb on the surface of MCNCs. Moreover, CDs are attached to the surface of MCNCs due to the complexation between the CDs and Fe^{3+} ions, and CDs are also embedded in the interior of the MCNCs when magnetic colloidal nanocrystals aggregate into clusters. These results give us a better understanding of the CD preparation and the architecture of MCNCs. Furthermore, upon the removal of Fe_3O_4, the CDs inside MCNCs could be released under a mild condition and the introduction of PEI could enhance the fluorescence intensity of CDs, which opens up the door for the application of bioresponsive off-on fluorescence *in vivo*.

We acknowledge the support from the National Science Foundation of China (Grant No. 51273047) and the "Shu Guang" Project (12SG07) supported by Shanghai Municipal Education Commission and Shanghai Education Development Foundation.

Notes and references

* State Key Laboratory of Molecular Engineering of Polymers and Department of Macromolecular Science, Fudan University, Shanghai 200433, China; Fax: +86 21-6564 0293; Tel: +86 21-6564 2385; E-mail: wlyang@fudan.edu.cn.

† Electronic Supplementary Information (ESI) available: [Experimental Section, Figure S1 to S9, and Table S1]. See DOI: 10.1039/c000000x/

1. Y. Fang, S. Guo, D. Li, C. Zhu, W. Ren, S. Dong and E. Wang, *ACS Nano*, 2012, **6**, 400-409.
2. S. Sahu, B. Behera, T. K. Maiti and S. Mohapatra, *Chem. Commun.* , 2012, **48**, 8835-8837.
3. B. Kong, A. Zhu, C. Ding, X. Zhao, B. Li and Y. Tian, *Adv. Mater.* , 2012, **24**, 5844-5848.
4. Y. Li, Y. Hu, Y. Zhao, G. Shi, L. Deng, Y. Hou and L. Qu, *Adv. Mater.* , 2011, **23**, 776-780.
5. V. Gupta, N. Chaudhary, R. Srivastava, G. D. Sharma, R. Bhardwaj and S. Chand, *J. Am. Chem. Soc.* , 2011, **133**, 9960-9963.
6. J. Zhao, G. Chen, L. Zhu and G. Li, *Electrochem. Commun.* , 2011, **13**, 31-33.
7. S. Zhuo, M. Shao and S.-T. Lee, *ACS Nano*, 2012, **6**, 1059-1064.
8. Y. P. Sun, B. Zhou, Y. Lin, W. Wang, K. A. S. Fernando, P. Pathak, M. J. Meziani, B. A. Harruff, X. Wang, H. F. Wang, P. J. G. Luo, H. Yang, M. E. Kose, B. L. Chen, L. M. Veca and S. Y. Xie, *J. Am. Chem. Soc.* , 2006, **128**, 7756-7757.
9. S. N. Baker and G. A. Baker, *Angew. Chem. Int. Ed.* , 2010, **49**, 6726-6744.
10. S. J. Zhu, Q. N. Meng, L. Wang, J. H. Zhang, Y. B. Song, H. Jin, K. Zhang, H. C. Sun, H. Y. Wang and B. Yang, *Angew. Chem. Int. Ed.* , 2013, **52**, 3953-3957.
11. W. Li, Z. Zhang, B. Kong, S. Feng, J. Wang, L. Wang, J. Yang, F. Zhang, P. Wu and D. Zhao, *Angew. Chem. Int. Ed.* , 2013, **52**, 8151-8155.
12. Y. Dong, H. Pang, H. B. Yang, C. Guo, J. Shao, Y. Chi, C. M. Li and T. Yu, *Angew. Chem. Int. Ed.* , 2013, **52**, 7800-7804.

13. B. Zhang, C.-y. Liu and Y. Liu, *Eur. J. Inorg. Chem.* , 2010, **2010**, 4411-4414.
14. M. Chen, W. Wang and X. Wu, *J. Mater. Chem. B*, 2014, **2**, 3937.
15. J. Guo, W. Yang and C. Wang, *Adv. Mater.* , 2013, **25**, 5196-5214.
16. J. Liu, Z. Sun, Y. Deng, Y. Zou, C. Li, X. Guo, L. Xiong, Y. Gao, F. Li and D. Zhao, *Angew. Chem. Int. Ed.* , 2009, **48**, 5875-5879.
17. H. Liu, T. Ye and C. Mao, *Angew. Chem. Int. Ed.* , 2007, **46**, 6473-6475.
18. S. Liu, J. Tian, L. Wang, Y. Zhang, X. Qin, Y. Luo, A. M. Asiri, A. O. Al-Youbi and X. Sun, *Adv. Mater.* , 2012, **24**, 2037-2041.
19. H. B. Na, G. Palui, J. T. Rosenberg, X. Ji, S. C. Grant and H. Mattoussi, *ACS Nano*, 2012, **6**, 389-399.
20. Y. Liu, T. Chen, C. Wu, L. Qiu, R. Hu, J. Li, S. Cansiz, L. Zhang, C. Cui, G. Zhu, M. You, T. Zhang and W. Tan, *J. Am. Chem. Soc.* , 2014, **136**, 12552-12555.
21. S. Xuan, Y.-X. J. Wang, J. C. Yu and K. Cham-Fai Leung, *Chem. Mater.* , 2009, **21**, 5079-5087.

